Gain and temperature in a slit nozzle supersonic chemical oxygen-iodine laser with transonic and supersonic injection of iodine

S. Rosenwaks, B. D. Barmashenko, E. Bruins, D. Furman, V. Rybalkin and A. Katz
Department of Physics, Ben-Gurion University of the Negev, Beer-Sheva 84105, Israel

ABSTRACT

Spatial distributions of the gain and temperature across the flow were studied for transonic and supersonic schemes of the iodine injection in a slit nozzle supersonic chemical oxygen-iodine laser as a function of the iodine and secondary nitrogen flow rate, jet penetration parameter and gas pumping rate. The mixing efficiency for supersonic injection of iodine (~ 0.85) is found to be much larger than for transonic injection (~ 0.5), the maximum values of the gain being ~ 0.65%/cm for both injection schemes. Measurements of the gain distribution as a function of the iodine molar flow rate nI_2 were carried out. For transonic injection the optimal value of nI_2 at the flow centerline is smaller than that at the off axis location. The temperature is distributed homogeneously across the flow, increasing only in the narrow boundary layers near the walls. Opening a leak downstream of the cavity in order to decrease the Mach number results in a decrease of the gain and increase of the temperature. The mixing efficiency in this case (~ 0.8) is much larger than for closed leak.

Keywords: chemical lasers, oxygen, iodine, power lasers

1. INTRODUCTION

The chemical oxygen-iodine laser (COIL)[1] emits at 1.315μm and is the shortest wavelength and the most efficient high–power chemical laser operating to date. The laser operation is based on the transition between the spin-orbit levels of the ground state configuration of the iodine atom, $I(5p^5\ ^2P_{1/2}) \rightarrow I(5p^5\ ^2P_{3/2})$, where the upper level is populated by a near resonant energy transfer from an $O_2(a^1\Delta_g)$ molecule (produced in a chemical generator by the reaction of gaseous chlorine with basic hydrogen peroxide solution):

$$O_2(^1\Delta) + I(^2P_{3/2}) \rightarrow O_2(^3\Sigma) + I(^2P_{1/2}). \qquad (1)$$

Mixing of the $O_2(^1\Delta)$ with I_2 molecules results in their dissociation to iodine atoms which are subsequently excited via reaction (1). Maximum values of lasing power were obtained for supersonic COILs where the primary gas ($O_2(^3\Sigma)$ - $O_2(^1\Delta)$ - He (N_2)) was brought to supersonic velocity via expansion in a converging-diverging nozzle [2], whereas the secondary I_2 – He (N_2) flow was injected into the primary flow at some location in the nozzle, either in the subsonic, transonic, or supersonic section of the flow.

One of the most important parameters of the supersonic COIL is the mixing efficiency η_{mix}, defined as the fraction of $O_2(^1\Delta)$ mixed with iodine (see below). To achieve high lasing power P this parameter should be high. Indeed, P can be estimated with the aid of the COIL heuristic equation [3]

$$P = 91(\text{kJ/mole})n\text{Cl}_2 U(Y_{plen} - Y_{diss} - Y_{th})\eta_{mix}\eta_{ext}, \qquad (2)$$

where 91(KJ/mole) is the energy of $I^*(\equiv I(^2P_{1/2}))$, $n\text{Cl}_2$ the chlorine molar flow rate, U the chlorine utilization and Y_{plen} is the $O_2(^1\Delta)$ yield just upstream of the iodine injection,

Gas and Chemical Lasers and Intense Beam Applications III, Steven J. Davis, Michael C. Heaven, Editors, Proceedings of SPIE Vol. 4631 (2002) © 2002 SPIE · 0277-786X/02/$15.00

$$Y_{diss} = NF\frac{n\mathrm{I}_2}{n\mathrm{Cl}_2\eta_{mix}} \qquad (3)$$

is the $O_2(^1\Delta)$ loss during iodine dissociation, η_{ext} the optical extraction efficiency of the resonator, F the iodine dissociation fraction and N is the number of $O_2(^1\Delta)$ molecules lost in the region of iodine dissociation per I_2 molecule. Eqs. (2) and (3) show that P increases with increasing η_{mix}. To estimate η_{mix} it is necessary to know the spatial distributions of the gain g and gas temperature T across the flow at the optical axis of the resonator. Both g and T can be easily measured using diode laser based diagnostic [4], the first measurements of the gain in supersonic COILs with subsonic injection of iodine being carried out in [5-7]. In [6] and [7] the gain distribution across the flow was monitored for the RADICL and VertiCOIL devices, 5 kW and 1 kW class supersonic COILs, respectively, developed at the Air Force Research Laboratory in Albuquerque, NM. These COILs use He as a buffer gas. For conditions where nitrogen buffer gas or no primary buffer gas is used, the subsonic mixing scheme is not optimal and it is reasonable to move the mixing point downstream to the transonic or supersonic part of the nozzle. This was done in [8, 9] where efficient supersonic COILs using N_2 buffer gas and applying transonic and supersonic mixing of iodine and oxygen were developed.

Recently we reported on the measurements of the gain and temperature at the flow centerline of a slit nozzle supersonic COIL operating without primary buffer gas and using transonic and supersonic schemes of iodine injection[10]. Comparison between the values of the gain at the flow centerline and at a point located lower than the flow centerline for transonic injection showed that the gain is strongly non-uniform in a direction perpendicular to both the flow direction and the optical axis, which means that the overall mixing is poor. To study the O_2/I_2 mixing in supersonic COILs with transonic and supersonic schemes of the iodine injection, we measured in the present work the spatial distributions of the gain and temperature as a function of the iodine and secondary nitrogen flow rate, jet penetration parameter and gas pumping rate. Using spatial distributions of g and T and the values of Y_{plen} , measured in the subsonic section of the flow as described in [11], we estimated the mixing efficiency η_{mix}. Flow conditions for good mixing in the COIL are found.

2. EXPERIMENTAL SETUP

The experimental setup, including a jet-type singlet oxygen generator (JSOG), is similar to that used in [10]. A brief description will be given here for completeness. The oxygen produced in the generator (the same as described in [10]) flows into a diagnostic cell with a flow cross section of 1 x 5 cm^2, which serves as an interface between the generator and the iodine injectors housing. The $O_2(^1\Delta)$ yield Y_{plen}, water vapor fraction, Cl_2 utilization and the temperature of the subsonic flow are simultaneously measured in the diagnostic cell as described in [11].

The iodine-oxygen mixing system is located downstream of the diagnostic cell and uses slit supersonic nozzle. We study three slit nozzles (Fig. 1) with iodine injection in the transonic (nozzle No. 1) and supersonic (nozzles No. 2 and 3) sections of the nozzle. All the slit nozzles have the same critical cross sections of 2.5 cm^2. In slit nozzle No. 1 iodine is injected at the nozzle throat (Fig. 1 a) and in nozzles No. 2 and 3 – in the supersonic section of the nozzle (Fig. 1 b and c). Nozzles 1 and 2 have two rows of injection holes in each wall (top and bottom). The first row of nozzle No. 1 has 31, 0.6-mm diameter holes and the second row 62, 0.4-mm diameter holes (this nozzle was referred to as nozzle No. 2 in [10]). The first row of nozzle No. 2 is located 3 mm downstream of the critical cross section and has 49, 0.5-mm diameter holes. The second row has 50, 0.4-mm diameter holes (this nozzle was referred to as nozzle No. 3 in [10]). Nozzles No. 1 and No. 2 have the same total cross section of the injection holes equal to 0.32 cm^2. The angle between the directions of the primary and secondary flows is 90^0 and 74^0 for nozzles 1 and 2, respectively. In order to decrease the effect of chocking the primary flow by the secondary stream, smaller angle (45^0) between the directions of the primary and secondary stream is used in nozzle No. 3. This nozzle has one row of 25, 1.3-mm diameter holes, located 2 mm downstream of the critical cross section, in each wall. The total cross section of the injection holes is 0.64 cm^2, i.e., larger than for nozzles No. 1 and 2. That is why this nozzle usually operates with secondary N_2 flow rate larger than the primary gas flow rate, which means that the operation conditions of the ejector COIL [12] can be tested using nozzle No. 3.

The laser section starts at the nozzle exit plane (flow cross section of 5 x 1 cm^2) from where the floor and the ceiling diverge at an angle of 8°. The optical cavity is of 5 cm gain length. For the gain diagnostic system we replaced the laser mirrors by optical windows. The gain was measured at the optical axis of the resonator, 4.5 cm downstream of the nozzle exit plane.

The iodine diagnostic system used in the present work was developed by Physical Sciences Inc [4] and is described in detail in [10]. It is based on sensitive absorption spectroscopy by tunable near infrared diode laser monitoring the gain for the $I^*(5p^5\ ^2P_{1/2}, F=3) \rightarrow I(5p^5\ ^2P_{3/2}, F = 4)$ transition at 1315 nm. The diode laser beam makes a single pass through the gain region of the cavity (Fig. 2). To probe the gain distribution in the direction y perpendicular to both the flow direction x and the cavity optical axis z, a collimator launching the beam from the diagnostic system into the gain region is mounted on a linear stage moving in the y direction. The gain is monitored in 50 points uniformly distributed over the flow height H = 1.5 cm. After passing the gain region the beam is focused onto a photodiode. The laser frequency is scanned over the I transition, monitoring the gain profile. The temperature of the gas in the cavity is found from the Doppler linewidth $\Delta\nu_D$, the later being determined by fitting the Voigt function to the experimental gain profile as described in [10].

3. RESULTS AND DISCUSSION

In what follows spatial dependencies $g(y)$ and $T(y)$ are presented for different values of iodine molar flow rate $n\mathrm{I}_2$, jet penetration parameter (defined below), nozzle type and rate of pumping of the gas. Most of the measurements are done for two values of Cl_2 flow rates, $n\mathrm{Cl}_2$ ~ 12 and ~ 15 mmole/s. The mixing parameter η_{mix}, characterizing the quality of mixing in the flow, is defined and found for different flow conditions.

3.1. Jet penetration parameter

As shown in [13] changes of secondary nitrogen molar flow rate $(n\mathrm{N}_2)_s$ affect the depth of penetration of the N_2/I_2 jets into the primary flow. That means that the gain spatial profiles depend on the penetration parameter defined as [13]

$$\Pi = \frac{n_s}{n_p}\sqrt{\frac{\mu_s T_s p_p}{\mu_p T_p p_s}}, \qquad (4)$$

where n, μ and p are the molar flow rate, molecular weight and pressure, respectively, and the subscripts "p" and "s" indicate primary and secondary flow.

Fig. 3 shows $g(y)$ dependencies for nozzle No. 1 with transonic injection of iodine, for $n\mathrm{I}_2$ = 0.25, 0.28 and 0.36 mmole/s and Π = 0.12, 0.16 and 0.18, respectively. Just as in [6], for small Π, 0.12 (underpenetrated jets), the gain distribution across the flow has bimodal structure with two peaks corresponding to the centerline of the jets and located higher and lower than the flow centerline. Increase of the penetration parameter results in merging of the two peaks and the gain distribution has one peak at the flow centerline. Π equal to 0.16 and 0.18 corresponds to full penetration (when the jets injected from the opposite walls touch and the bimodal structure disappears) and overpenetration of the jets, respectively. The gain distribution for the case of overpenetration is a little narrower than for full penetration, which is probably due to the effect of the overlap of the overpenetrated jets. The maximum gain at the flow centerline is achieved for overpenetrated jets.

3.2. Nozzle No. 1 with transonic injection of iodine

The $g(y)$ distributions for nozzle No. 1 for different values of $n\mathrm{I}_2$ are shown in Fig. 4a for overpenetrated jets (Π = 0.26, corresponding to maximum gain) and no primary N_2. The gain is a non-monotonous function of $n\mathrm{I}_2$ and the dependence of the gain on $n\mathrm{I}_2$ at the flow centerline is different from that at the off axis locations. Fig. 4b shows dependencies of g on $n\mathrm{I}_2$ at $y = 0$ (flow centerline) and y = 0.5 cm. It is seen that the optimal value of $n\mathrm{I}_2$ at the flow

centerline is smaller than that at the off centerline location. The reason for this behavior is that the initial I_2 distribution across the flow is strongly nonuniform, the iodine being concentrated near the flow centerline. For low values of the iodine flow rate, the dissociation rate is proportional to the iodine density, hence at the flow centerline both dissociation and gain increase faster with increasing nI_2 than at the off axis location. For higher iodine flow rates the excited species, $O_2(^1\Delta)$, I* and I_2*, are rapidly quenched by iodine molecules which results in a decrease of the gain. The quenching rate, which is proportional to the density of I_2, is higher at the flow centerline than at the off axis location, resulting in faster decrease of the gain at the flow centerline for large iodine flow rate. Therefore the optimal nI_2 at the flow centerline is smaller than at the off axis location.

The *T(y)* dependencies are shown in Fig. 5a and 5b for the cases of overpenetration and underpenetration, respectively. It is seen that the temperature is distributed homogeneously across the flow for different values of the penetration parameter, increasing only in the narrow boundary layers near the walls. The fact that the temperature distribution is much more homogeneous than the gain distribution, can probably be explained by the high rate of the heat transfer across the flow. The same homogeneous temperature distributions for transonic injection are also observed for different values of the flow parameters.

Using the dependencies *g(y)* and *T(y)* it is possible to determine the distribution of the iodine atoms molar fraction $\chi_I(y)$ and to define the mixing parameter η_{mix}. Taking into account that the distance between the iodine injection holes is much smaller than the flow height we can assume that both the gain and temperature are uniform along the optical axis direction *z*. This assumption is confirmed by the fact that the intensity of the yellow emission of $I_2\left(B^3\Pi_0^+\right)$ molecules observed in the supersonic section of the flow is uniform along the *z* direction. In this case the relation between *g(y)*, *T(y)*, $\chi_I(y)$ and $O_2(^1\Delta)$ yield *Y* is

$$g = \sigma_0 \left(\frac{300}{T}\right)^{1/2} \frac{p}{kT} \chi_I \frac{(2K_e+1)Y-1}{(K_e-1)Y+1}, \tag{5}$$

where σ_0 = 1.29 x10^{-17} cm^2 is the stimulated emission cross section at T = 300 K, p the pressure at the optical axis and K_e = 0.75 exp (402/T) is the equilibrium constant of reaction (1). For nI_2 much smaller than the optimal iodine flow rate we can assume that on the one hand the rate of iodine dissociation is proportional to the density of I_2 [13], which means that the molar fraction of I_2, $\chi_{I_2}(y)$, is proportional to $\chi_I(y)$, and on the other hand the yield *Y* is close to Y_{plen}, measured in the subsonic section of the flow. In this case $\chi_I(y)$ found from Eq. (5) (with $Y = Y_{plen}$) can be used to define η_{mix}:

$$\eta_{mix} \equiv \frac{\int_{-H/2}^{H/2} \chi_I(y)dy}{(\chi_I)_{\max} H}, \tag{6}$$

where $(\chi_I)_{\max}$ is the maximum value of $\chi_I(y)$. It should be noted once again that the definition (6) (with $\chi_I(y)$ calculated by (5)) makes sense only for small nI_2. Fig. 6 shows distributions of $g(y)/g_{max}$ and $\chi_I(y)/(\chi_I)_{\max}$ for the same flow conditions as in Fig. 4 at nI_2 = 0.228 mmole/s which is much smaller than the optimal nI_2 = 0.38 mmole/s. It is seen that for transonic injection the normalized distributions of g and χ_I are very close to each other, being different only near the duct walls. The calculated value of η_{mix} is equal to 0.52, close values of η_{mix} being found for other primary flow parameters and in particular for the primary flow diluted by N_2 buffer gas. Thus, poor mixing is achieved for transonic injection of iodine.

To increase the mixing efficiency it is necessary to decrease the pumping rate. This is achieved by opening a leak downstream of the cavity as explained in [10] and results in increase of the pressure and decrease of the Mach number in

the supersonic section of the flow. Figs. 7a and b show the *g(y)* distributions (at different nI_2) for opened and closed leak, respectively, and the same flow rates of Cl_2 and N_2. Figs. 8 a and b show *T(y)* for the same conditions. It is seen that maximum values of the gain at the flow centerline for opened leak are smaller than for closed leak, the gain distribution for opened leak being more homogeneous than for closed leak. This behavior is in agreement with the conclusions drawn in [10] using a simple theoretical model. The temperatures for opened leak are higher than for closed leak, which is due to weaker expansion of the gas for opened leak. Calculations of the mixing parameters using Eqs. (5) and (6) at $nI_2 \approx 0.23$ mmole/s show that η_{mix} is equal to 0.83 and 0.57 for opened and closed leak, respectively. Therefore for opened leak the mixing is much better than for closed leak, which is also in agreement with conclusions obtained in [10].

3.3. Nozzles No. 2 and 3 with supersonic injection of iodine

Figs. 9 a and b show the *g(y)* distributions for nozzles No. 2 and 3, respectively. The primary flow did not contain N_2 buffer gas and the leak downstream of the cavity was closed. Comparison between Fig. 4a and Figs. 9 a and b shows that the maximum values of the gain are almost the same for transonic and supersonic injection, however, for supersonic injection the gain is distributed much more uniformly across the flow. Fig. 10 shows calculated $\chi_I(y)/(\chi_I)_{max}$ for nozzle No. 3 at nI_2 = 0.39 mmole/s and the same flow conditions as in Fig. 9b. Comparison between Figs. 6 and 10 shows that unlike transonic injection, where iodine is concentrated near the centerline, for supersonic injection the iodine distribution across the flow is rather uniform and weakly increases near the walls. The calculated η_{mix} is 0.82 and 0.86 for nozzles No. 2 and 3, respectively. Hence for any angle of injection the supersonic injection scheme provides for much more uniform mixing than the transonic injection scheme.

4. SUMMARY

We measured spatial distributions of the gain and temperature across the flow in a slit nozzle supersonic COIL without primary buffer gas using diode laser based diagnostic systems. This was done to estimate the oxygen/iodine mixing efficiency of the COIL, which, in turn, strongly affects the output power. The spatial distributions of the gain and temperature were studied for transonic and supersonic schemes of the iodine injection as a function of the iodine and secondary nitrogen flow rate, jet penetration parameter and gas pumping rate. The mixing efficiency for supersonic injection of iodine (~ 0.8) is found to be much larger than for transonic injection (~ 0.5), the maximum values of the gain being ~ 0.65%/cm for both injection schemes. Measurements of the gain distribution as a function of the iodine molar flow rate nI_2 were carried out. For transonic injection the optimal value of nI_2 at the flow centerline is smaller than that at the off axis location. The temperature is distributed homogeneously across the flow, increasing only in the narrow boundary layers near the walls. Opening a leak downstream of the cavity in order to decrease the Mach number results in a decrease of the gain and increase of the temperature. The mixing efficiency in this case (~ 0.8) is much larger than for closed leak.

REFERENCES

1. W. E. McDermott, N. R. Pchelkin, D. J. Benard, R. R. Bousek, "An electronic transition chemical laser," *Appl. Phys. Lett.*, vol. 32, pp. 469-470, 1978.
2. K. A. Truesdell and S. E. Lamberson, "Phillips laboratory COIL technology overview," *SPIE*, vol.1810, pp. 476 - 492, 1992.
3. J. Hon, D. N. Plummer, P. G. Crowell, J. Erkkila, G. D. Hager, C. A. Helms, K. A. Truesdell, "Heuristic Method for Evaluating COIL Performance," *AIAA Journal*, vol. 43, pp.1595-1603, 1996.
4. S. J. Davis, M. G. Allen, W. J. Kessler, K. R. McManus, M. F. Miller and P. A. Mulhall, "Diode laser-based sensors for chemical oxygen-iodine lasers," *SPIE*, vol. 2702, pp. 195 – 201,1996.
5. E. Lebiush, B. D. Barmashenko, A. Elior and S. Rosenwaks, "Parametric study of the gain in a small scale, grid nozzle supersonic chemical oxygen-iodine laser," *IEEE J. Quantum Electronics*, vol.31, pp. 903-909, 1995.
6. R. F. Tate, B. S. Hunt, C. A. Helms, K. A. Truesdell and G. D. Hager, "Spatial gain measurements in a chemical oxygen iodine laser (COIL)," *IEEE J. Quantum Electronics*, vol.31, pp. 1632 - 1636, 1995.
7. P. B. Keating, B. A. Anderson, C. A. Helms, T. L. Rittenhouse, G. D. Hager and K. A. Truesdell, "2-D spatial gain maps in a small scale chemical oxygen-iodine laser," in *Proc. Int. Conf. Lasers '96*, Portland, OR, Dec. 1996.

8. D. Furman, B. D. Barmashenko and S. Rosenwaks, "An efficient supersonic chemical oxygen-iodine laser operating without buffer gas and with simple nozzle geometry," *Appl. Phys. Lett.*, vol. 70, pp. 2341-2343, 1997.
9. V. N. Azyazov, M. V. Zagidullin, V. D. Nikolaev and V. S. Safonov, "Chemical oxygen-iodine laser with mixing of supersonic jets," *Quantum Electronics*, vol. 27, pp. 491-494, 1997.
10. D. Furman, E. Bruins, V. Rybalkin, B. D. Barmashenko and S. Rosenwaks, "Parametric study of small signal gain in a slit nozzle, supersonic chemical oxygen - iodine laser operating without primary buffer gas," *IEEE J. Quantum Electronics*, vol. 37, pp. 174-182, 2001.
11. D. Furman, B. D. Barmashenko and S. Rosenwaks, "Diode-laser based absorption spectroscopy diagnostics of a jet-type generator for chemical oxygen-iodine lasers," *IEEE J. Quantum Electronics*, vol. 35, pp. 540-547, 1999.
12. T. T. Yang, Y. C. Hsia, L. F. Moon and R. A. Dickerson, "Advanced Mixing Nozzle Concepts for COIL," *SPIE* vol. 3931, pp. 116-130, 2000.
13. C. A. Helms, J. Shaw, G. D. Hager and K. A. Truesdell, "Iodine dissociation in COILs," *SPIE*, vol. 2502, pp. 250 – 257, 1996.

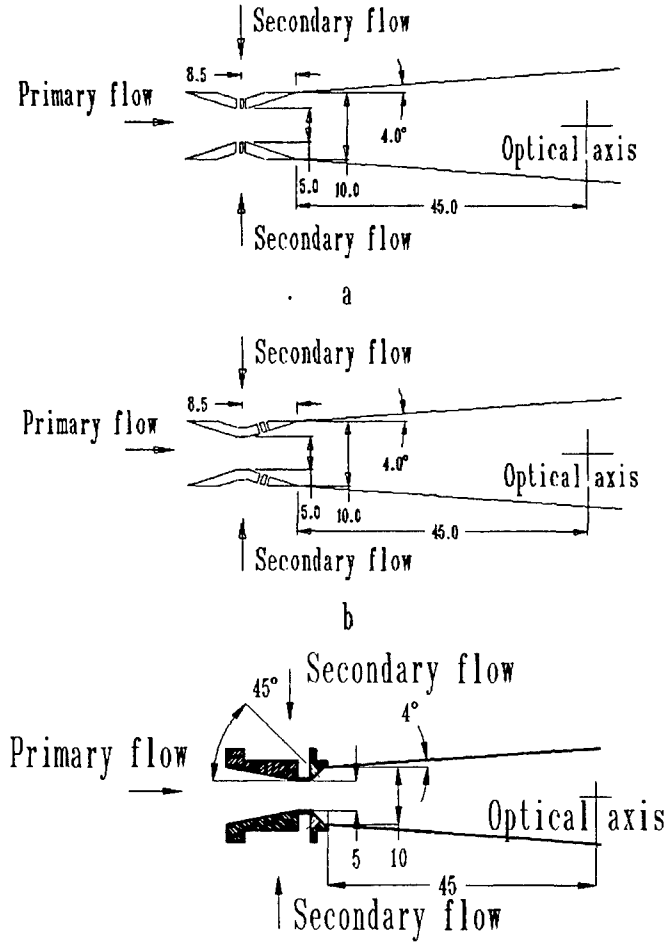

Fig. 1. Schematics of the slit nozzles; a) slit nozzle No. 1 with transonic injection of I_2; b) and c) slit nozzles No. 2 and 3, respectively, with supersonic injection of iodine. All measures are in millimeters.

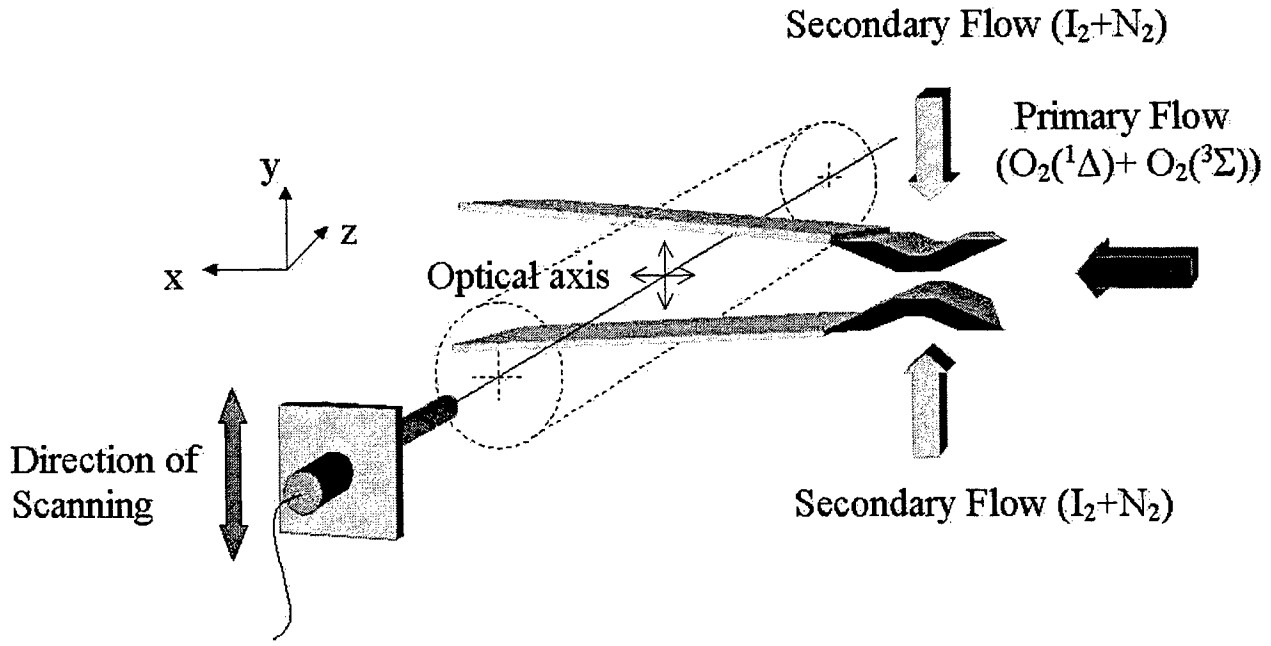

Fig. 2. Schematics of the gain scanning experiment.

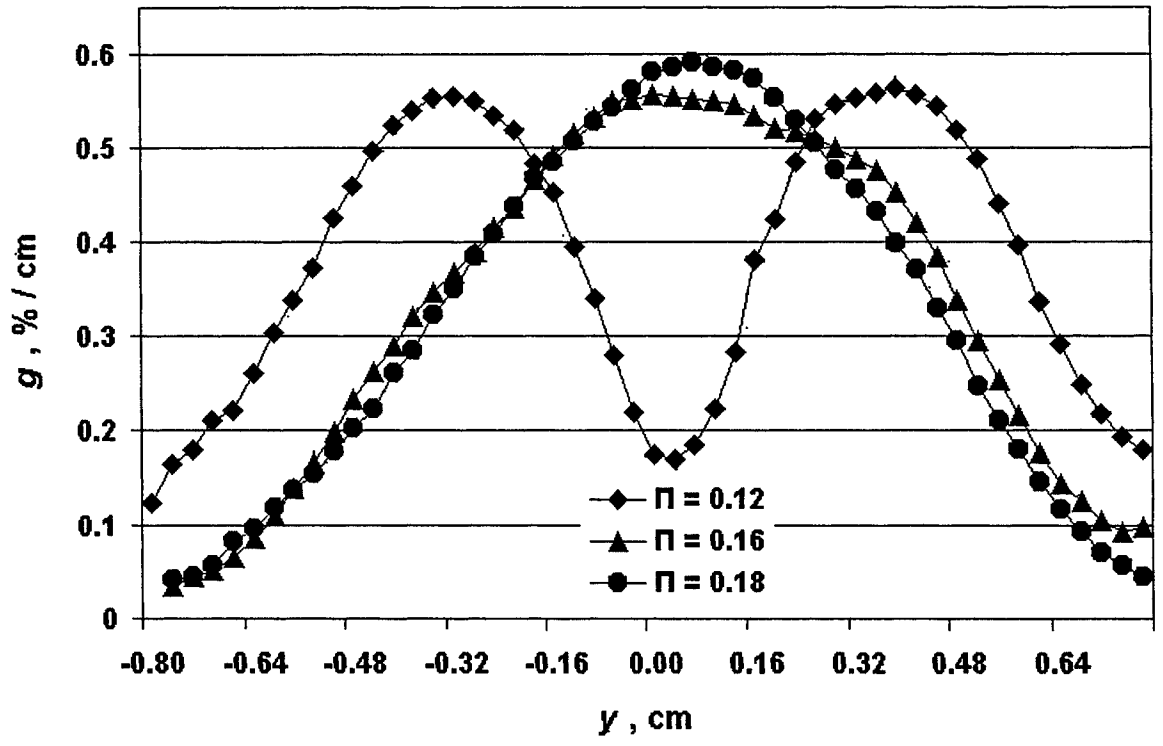

Fig. 3. The gain distributions across the flow, for nI_2 = 0.25, 0.28 and 0.36 mmole/s and penetration parameter Π = 0.12, 0.16 and 0.18, respectively, for nozzle No. 1 (transonic injection). The chlorine and primary nitrogen flow rates are 14.8 and 15.2 mmole/s, respectively.

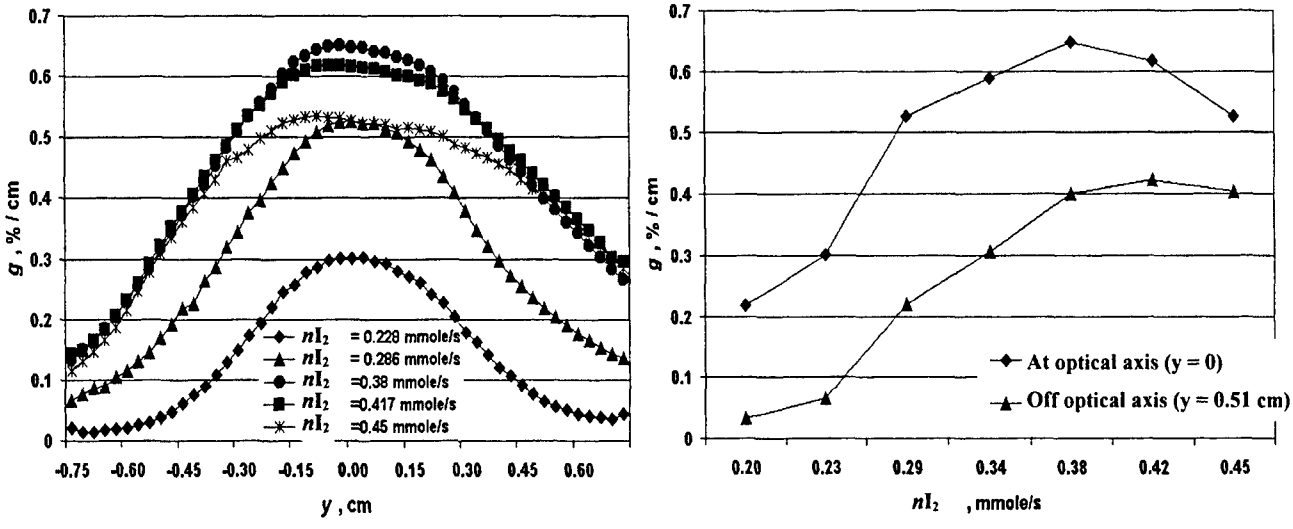

Fig. 4. (a) The gain distributions across the flow for different values of nI_2 for nozzle No. 1 (transonic injection); the chlorine, primary and secondary nitrogen flow rates are 14.4, 0 and 9.9 mmole/s, respectively, the penetration parameter $\Pi = 0.26$; (b) the gain dependencies on nI_2 at the optical axis and off the optical axis for the same flow conditions as in (a).

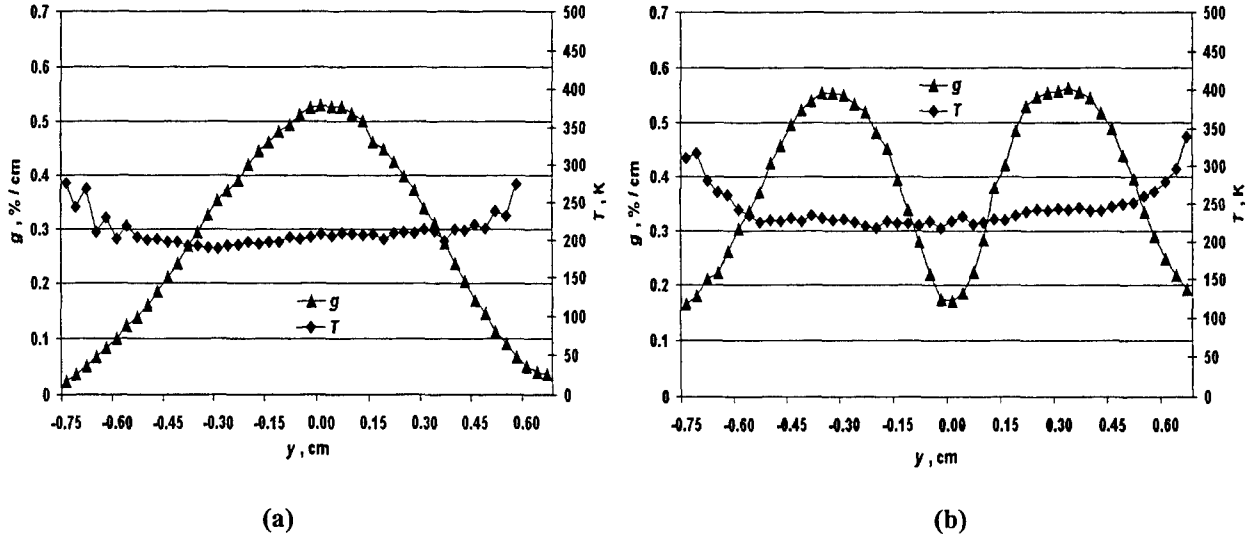

Fig. 5. The gain and temperature distributions across the flow for nozzle No. 1 (transonic injection), the chlorine, primary nitrogen and iodine flow rates are 14.8, 15.2, and 0.25 mmole/s, respectively; (a) overpenetrated jets, the penetration parameter $\Pi = 0.18$ and the secondary flow rate is 12.6 mmole/s; (b) underpenetrated jets, $\Pi = 0.12$; the secondary nitrogen flow rate is 6.4 mmole/s.

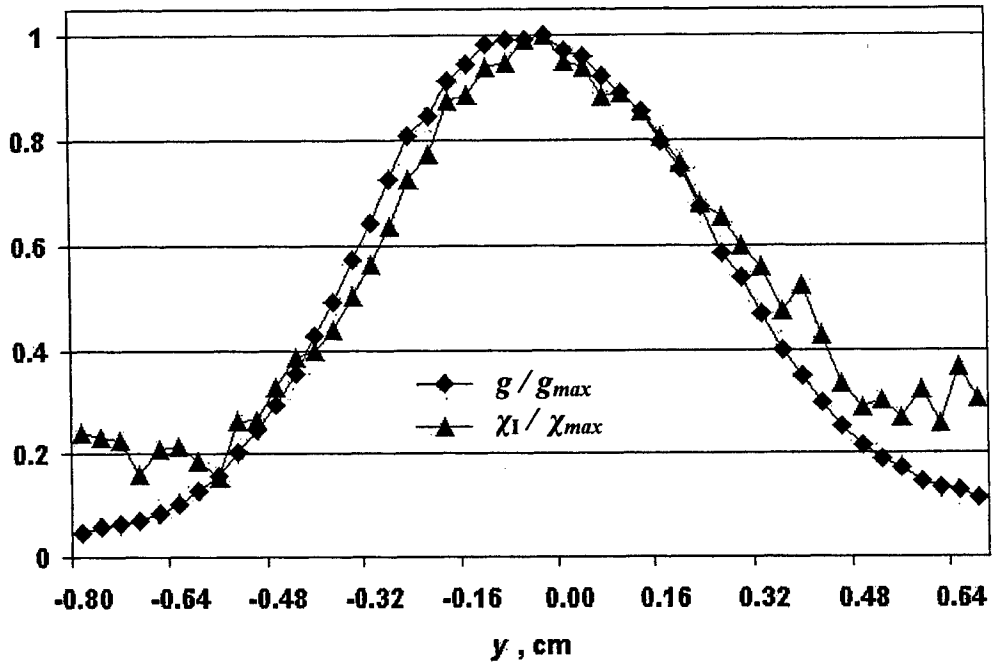

Fig. 6. Normalized gain $g(y)/g_{max}$ and iodine atoms molar fraction $\chi_I(y)/(\chi_I)_{max}$ across the flow for nozzle No. 1 (transonic injection) and the same flow conditions as in Fig. 4 and $nI_2 = 0.23$ mmole/s.

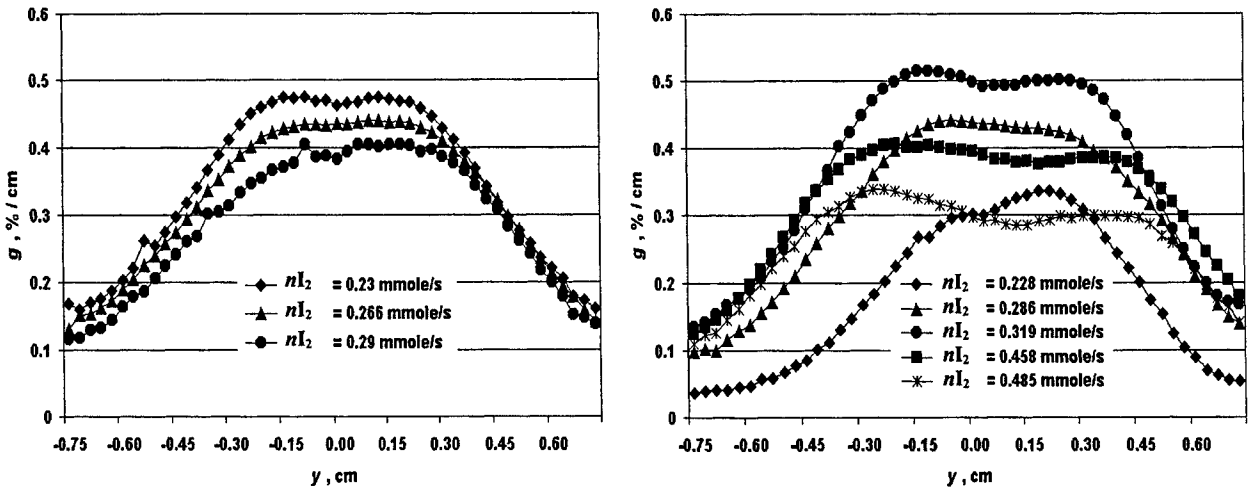

(a) (b)

Fig. 7. The gain distribution across the flow for nozzle No.1 (transonic injection) with opened (a) and closed (b) leak downstream of the cavity; (a) the chlorine, primary and secondary nitrogen flow rates are 11.8, 0, and 4.1 mmole/s, respectively; (b) the chlorine, primary and secondary nitrogen flow rates are 14.3, 0, and 4.9 mmole/s, respectively. For both opened and closed leak the penetration parameter Π is the same (0.19).

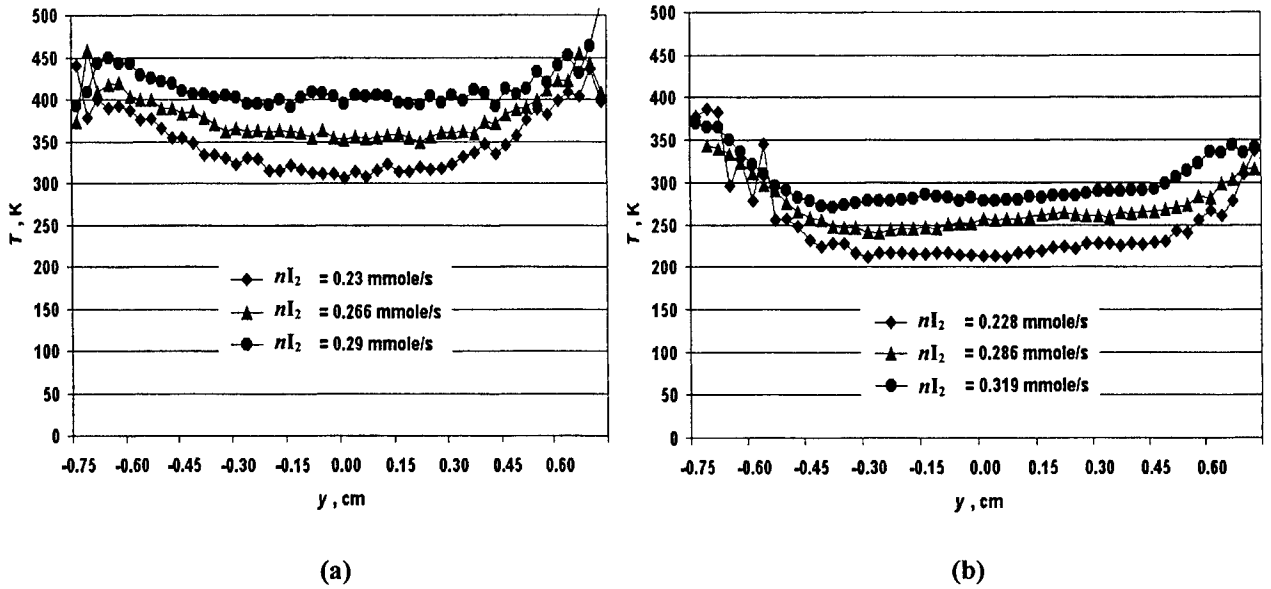

Fig. 8. The temperature distribution across the flow for nozzle No.1 (transonic injection) with opened (a) and closed (b) leak downstream of the cavity and the same flow conditions as in Fig. 7.

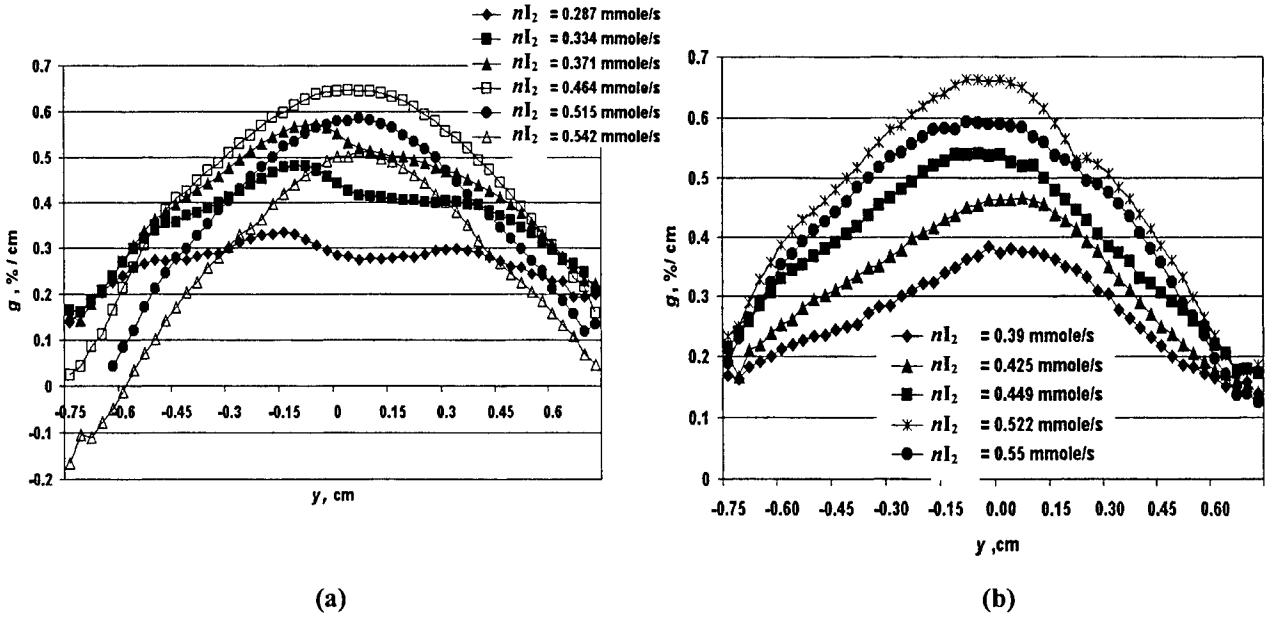

Fig. 9. The gain distributions across the flow for different values of nI_2 and closed leak for nozzles No. 2 (a) and 3 (b) (supersonic injection); (a) the chlorine, primary and secondary nitrogen flow rates are 15.1, 0 and 12.7 mmole/s, respectively; (b) the chlorine, primary and secondary nitrogen flow rates are 15, 0 and 20.2 mmole/s, respectively.

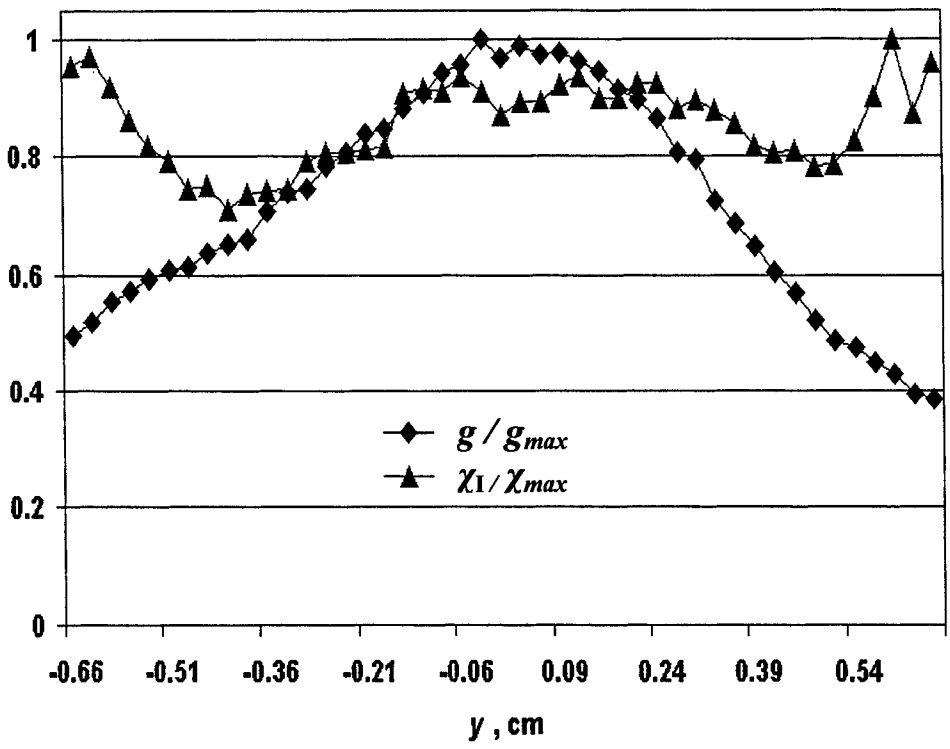

Fig. 10. Normalized gain $g(y)/g_{max}$ and iodine atoms molar fraction $\chi_I(y)/(\chi_I)_{max}$ across the flow for nozzle No .3 (supersonic injection) and the same flow conditions as in Fig. 9b and $nI_2 = 0.39$ mmole/s.